Electronic supplementary information

Facile synthesis of high-performance nonfullerene acceptor isomers *via* a one stone two birds strategy

Tengfei Li,[a] Langxuan Yang,[a] Yiqun Xiao,[b] Kuan Liu,[a] Jiayu Wang,[a] Xinhui Lu,[b] and Xiaowei Zhan [a,*]

Materials

Unless stated otherwise, all the solvents and chemical reagents used were obtained commercially and used without further purification. Toluene and THF were distilled from sodium benzophenone under nitrogen before use. Compound **1**,[S1] 2FIC[S2] and 3TT[S3] were synthesized according to our reported procedures. PTB7-Th (M_w = 124 kDa, M_w/M_n = 1.7) was purchased from 1-materials Inc. Zinc acetate dihydrate, ethanolamine and MoO_3 were obtained from Aldrich Inc.

Synthesis

3TT-SnMe$_3$. To a solution of 3TT (216 mg, 0.2 mmol) in THF (30 mL) at −78 ºC was added 1.6 M *n*-butyllithium in hexane (0.16 mL, 0.25 mmol) dropwise under nitrogen. The mixture was stirred at −78 ºC for 1.5 h, and then 1.0 M trimethyltin chloride in THF (0.25 mL, 0.25 mmol) was added. The mixture was stirred overnight at room temperature. Brine (30 mL) was added and the mixture was extracted with dichloromethane (2 × 30 mL). The organic phase was dried over anhydrous $MgSO_4$ and filtered. After removing the solvent from the filtrate, the residue was poured into methanol (100 mL) and filtered yielding an orange solid (crude product: 172 mg, 69%). The product was directly used for next step reaction without further purification due to poor stability in air.

Compound 2. To a three-necked round bottom flask were added 3TT-$SnMe_3$ (373 mg, 0.3 mmol), compound **1** (88 mg, 0.3 mmol) and toluene (30 mL). The mixture was deoxygenated with nitrogen for 15 min. $Pd(PPh_3)_4$ (18 mg, 0.015 mmol) was added under nitrogen. The mixture was refluxed for 48 h and then cooled down to room temperature. Water (40 mL) was added and the mixture was extracted with dichloromethane (2 × 40 mL). The organic phase was dried over anhydrous $MgSO_4$ and filtered. After removing the solvent from the filtrate, the residue was purified by column chromatography on silica gel using petroleum ether/dichloromethane (4:1) as the eluent yielding a red solid (256 mg, 66%). ^{1}H NMR (400 MHz, CD_2Cl_2): δ 7.83 (s, 1H), 7.47 (d, J = 5.2 Hz, 1H), 7.29 (m, 2H), 7.22 (d, J = 5.2 Hz, 1H), 7.14 (m, 16H), 4.34 (m, 2H), 2.54 (t, J = 8.0 Hz, 8H), 1.54 (m, 8H), 1.33 (m, 3H), 1.26 (m, 24H), 0.83 (m, 12H). ^{13}C NMR (100 MHz, CD_2Cl_2): δ 161.86, 148.94, 148.07, 147.44, 145.05, 142.62, 142.53, 142.46, 141.29, 140.83, 140.29, 138.78, 138.16, 138.06, 137.91, 137.88, 135.59, 135.33, 134.74, 134.32, 133.78, 129.26, 128.84, 128.76, 128.72, 127.81, 125.97, 122.88, 120.42, 120.28, 118.79, 62.25, 61.30, 35.54, 31.68, 31.35, 29.15, 22.58, 14.05, 13.84. MS (MALDI-TOF): m/z 1291.1 (M^+). Anal. calc. for $C_{77}H_{78}O_2S_8$: C, 71.58; H, 6.09. Found: C, 71.69; H, 6.01.

4TT. To a suspension of magnesium turnings (72 mg, 3 mmol) and a piece of iodine in dry THF (5 mL) was added 1-bromo-4-hexylbenzene (720 mg, 3 mmol) dropwise under nitrogen, and then the mixture was stirred for 2 h. To a solution of compound **2** (645 mg, 0.5 mmol) in dry THF (20 mL) was added the prepared Grignard reagent dropwise at room temperature under nitrogen. The mixture was stirred at reflux for 12 h and then cooled down to room temperature. A saturated NH_4Cl aqueous solution (40 mL) was added and the mixture was extracted with chloroform (2 × 40 mL). The organic phase was dried over anhydrous

$MgSO_4$ and filtered. After removing the solvent, the orange residue was resolved by octane (30 mL) and acetic acid (10 mL), then concentrated H_2SO_4 (0.05 mL) was added dropwise, the mixture was stirred at reflux for 12 h and then quenched with water. The organic layer was washed with water for three times and extracted with dichloromethane (2 × 30 mL), and was dried over anhydrous $MgSO_4$ and filtered. After removing the solvent from the filtrate, the residue was purified by column chromatography on silica gel using petroleum ether/dichloromethane (50:1) as the eluent yielding an orange solid (543 mg, 70%). ^{1}H NMR (400 MHz, CD_2Cl_2): δ 7.10 (m, 24H), 7.01 (m, 4H), 2.56 (m, 4H), 2.54 (m, 8H), 1.55 (m, 12H), 1.27 (m, 36H), 0.83 (m, 18H). ^{13}C NMR (150 MHz, $CDCl_3$): δ 148.10, 147.05, 142.28, 142.17, 140.49, 139.02, 138.52, 138.46, 137.89, 135.00, 134.23, 128.88, 128.80, 128.18, 128.10, 125.68, 120.31, 62.38, 35.76, 31.82, 31.31, 29.30, 22.70, 14.20. MS (MALDI-TOF): *m/z* 1551.2 (M^+). Anal. calc. for $C_{99}H_{106}S_8$: C, 76.59; H, 6.88. Found: C, 76.78; H, 6.79.

4TT-CHO and *i*-4TT-CHO. 4TT (232 mg, 0.15 mmol), $POCl_3$ (0.6 mL) and DMF (3 mL) were added to 1,2-dichloroethane solution (15 mL) under the protection of nitrogen at room temperature. After stirring at 85 °C for 12 h, the mixture was quenched with 5 mL saturated CH_3COONa (aq) and extracted with chloroform (2 × 30 mL). The organic phase was dried over anhydrous $MgSO_4$ and filtered. After removing the solvent from the filtrate, the residue was purified by column chromatography on silica gel using petroleum ether/dichloromethane (4:1) as the eluent yielding a mixture of red solids (total yield: 185 mg, 77%).

To study the components and chemical structures of the mixture, we separated the mixture by further running column chromatography on silica gel using petroleum ether/dichloromethane (4:1) to afford two pure aldehydes (42% 4TT-CHO and 58% *i*-4TT-CHO in the mixture).

For 4TT-CHO, ^{1}H NMR (400 MHz, CD_2Cl_2): δ 9.86 (s, 2H), 7.90 (s, 2H), 7.15 (m, 8H), 7.10 (m, 16H), 2.55 (m, 12H), 1.57 (m, 12H), 1.28 (m, 36H), 0.85 (m, 18H). ^{13}C NMR (150 MHz, $CDCl_3$): δ 182.54, 150.97, 148.40, 143.22, 142.68, 142.59, 140.55, 140.15, 139.41, 138.00, 137.46, 136.75, 129.82, 129.04, 128.99, 128.02, 127.84, 101.98, 62.33, 35.70, 31.77, 29.80, 29.22, 22.65, 14.15. MS (MALDI-TOF): *m/z* 1608.3 (MH^+). Anal. calc. for $C_{101}H_{106}O_2S_8$: C, 75.42; H, 6.64. Found: C, 75.64; H, 6.59.

For *i*-4TT-CHO, ^{1}H NMR (400 MHz, CD_2Cl_2): δ 9.86 (s, 1H), 9.83 (s, 1H), 7.90 (s, 1H), 7.79 (s, 1H), 7.12 (m, 20H), 7.01 (m, 4H), 2.58 (m, 12H), 1.60 (m, 12H), 1.29 (m, 36H), 0.87 (m, 18H). ^{13}C NMR (100 MHz, CD_2Cl_2): δ 183.23, 182.63, 151.01, 148.69, 148.29, 147.59, 145.65, 143.35, 142.75, 142.55, 142.07, 140.55, 140.23, 139.79, 138.53, 137.93, 137.50, 136.79, 135.28, 134.00, 129.91, 129.39, 129.10, 129.02, 128.85, 127.94, 127.89, 120.76, 62.50, 49.24, 35.78, 37.75, 31.84, 31.83, 31.34, 29.33, 29.27, 29.14, 22.75, 22.72, 14.23, 14.21. MS (MALDI-TOF): *m/z* 1608.0 (MH^+). Anal. calc. for $C_{101}H_{106}O_2S_8$: C, 75.42; H, 6.64. Found: C, 75.58; H, 6.61.

We further changed the synthetic conditions to see if we could control the selectivity of formylation on 4TT unit.

When 4TT (232 mg, 0.15 mmol) was added to Vilsmeier reagent prepared with $POCl_3$ (0.6 mL) in DMF (3 mL) in 1,2-dichloroethane solution at 0 °C under the protection of nitrogen, then the solution was stirred at 75 °C for 12 h, the product was mainly 4TT-CHO (241 mg, 74%).

In another way, a solution of 4TT (232 mg, 0.15 mmol) in THF (20 mL) at −78 ºC was added 1.6 M *n*-butyllithium in hexane (0.2 mL, 0.32 mmol) dropwise under nitrogen. The mixture was stirred at −78 ^{o}C for 1.5 h, and then at least 23.5 mg (0.32 mmol) anhydrous DMF was added. The mixture was stirred overnight at room temperature. Brine (30 mL) was added and the mixture was extracted with chloroform (2 × 30 mL). The organic phase was

dried over anhydrous $MgSO_4$ and filtered. After removing the solvent from the filtrate, the residue was purified by column chromatography on silica gel using petroleum ether/dichloromethane (4:1) as the eluent yielding two red solids (125 mg, 52% for 4TT-CHO; 55 mg, 23% for *i*-4TT-CHO).

FUIC and *i*-FUIC. To a three-necked round bottom flask were added the mixture aldehydes (161 mg, 0.1 mmol), 2FIC (92 mg, 0.4 mmol), pyridine (0.5 mL) and chloroform (20 mL). The mixture was deoxygenated with nitrogen for 15 min and then stirred at reflux for 12 h. After cooling to room temperature, the mixture was poured into methanol (200 mL) and filtered. The residue was purified by column chromatography on silica gel using petroleum ether/dichloromethane (1:1) as eluent yielding two purple solids (59 mg for FUIC, 75 mg for *i*-FUIC, total yield: 66%).

For FUIC, ^{1}H NMR (400 MHz, $CDCl_3$): δ 8.79 (s, 2H), 8.49 (m, 2H), 8.09 (s, 2H), 7.64 (m, 2H), 7.16 (m, 24H), 2.56 (m, 12H), 1.55 (m, 12H), 1.28 (m, 36H), 0.85 (m, 18H). ^{13}C NMR (100 MHz, $CDCl_3$): δ 185.95, 158.14, 155.59, 153.53, 151.20, 149.14, 148.27, 147.53, 143.03, 142.89, 142.72, 141.17, 138.54, 137.89, 137.75, 137.50, 136.96, 136.65, 135.85, 134.44, 129.23, 127.85, 120.43, 114.65, 114.54, 112.61, 112.42, 68.55, 62.47, 35.70, 31.76, 31.29, 29.24, 22.65, 14.15. MS (MALDI-TOF): *m/z* 2033.3 (MH^+). Anal. calc. for $C_{125}H_{110}F_4N_4O_2S_8$: C, 73.86; H, 5.45; N, 2.76. Found: C, 73.99; H, 5.38; N, 2.79.

For *i*-FUIC, ^{1}H NMR (400 MHz, CD_2Cl_2): δ 8.80 (s, 1H), 8.69 (s, 1H), 8.49 (m, 2H), 8.16 (s, 1H), 8.11 (s, 1H), 7.64 (m, 2H), 7.15 (m, 20H), 7.05 (m, 4H), 2.56 (m, 12H), 1.64 (m, 12H), 1.25 (m, 36H), 0.83 (m, 18H). ^{13}C NMR (100 MHz, $CDCl_3$): δ 186.03, 185.11, 158.39, 156.49, 153.67, 153.23, 151.32, 149.09, 148.37, 147.65, 143.62, 143.05, 142.79, 142.36, 142.31, 141.23, 140.55, 140.47, 138.67, 138.59, 138.39, 138.34, 138.28, 138.00, 137.58, 137.40, 137.07, 136.12, 135.73, 135.68, 135.18, 134.33, 129.51, 129.28, 129.14, 129.02,

127.92, 127.87, 122.48, 121.29, 120.59, 115.14, 114.73, 114.65, 114.37, 114.17, 112.66, 70.08, 68.65, 62.56, 62.46, 49.45, 35.80, 31.92, 31.83, 31.53, 31.36, 31.33, 29.33, 29.20, 22.77, 22.73, 22.72, 14.22. MS (MALDI-TOF): *m/z* 2032.5 (M^+). Anal. calc. for $C_{125}H_{110}F_4N_4O_2S_8$: C, 73.86; H, 5.45; N, 2.76. Found: C, 74.11; H, 5.25; N, 2.69.

To understand effect of the aldehyde isomeric mixture on yields of final products FUIC and *i*-FUIC, we also used pure 4TT-CHO / *i*-4TT-CHO to react with 2FIC.

FUIC. To a three-necked round bottom flask were added 4TT-CHO (161 mg, 0.1 mmol), 2FIC (92 mg, 0.4 mmol), pyridine (0.5 mL) and chloroform (20 mL). The mixture was deoxygenated with nitrogen for 15 min and then stirred at reflux for 12 h. After cooling to room temperature, the mixture was poured into methanol (200 mL) and filtered. The residue was purified by column chromatography on silica gel using petroleum ether/dichloromethane (1:1) as eluent yielding a purple solid (142 mg, 70%).

***i*-FUIC.** To a three-necked round bottom flask were added *i*-4TT-CHO (161 mg, 0.1 mmol), 2FIC (92 mg, 0.4 mmol), pyridine (0.5 mL) and chloroform (20 mL). The mixture was deoxygenated with nitrogen for 30 min and then stirred at reflux for 12 h. After cooling to room temperature, the mixture was poured into methanol (200 mL) and filtered. The residue was purified by column chromatography on silica gel using petroleum ether/dichloromethane (1:1) as eluent yielding a purple solid (128 mg, 63%).

The final step reaction using either the aldehyde isomeric mixture or pure isomer afforded similar total yields of **FUIC** and ***i*-FUIC**.

Instruments and measurements

The ^1H and ^{13}C NMR spectra were recorded using Bruker AVANCE 400 MHz and 600 MHz spectrometer. Mass spectra were recorded using AB Sciex 5800 MALDI-TOF Analyzer in the MALDI mode. Elemental analysis was performed using a Flash EA1112 analyzer. UV-

vis absorption spectra (solution in chloroform, thin film using quartz substrate) was measured using a JΛSCO V-570 spectrophotometer. Electrochemical measurements were carried out under nitrogen in a solution of tetra-n-butylammonium hexafluorophosphate ($[^nBu_4N]^+[PF_6]^-$) (0.1 M) in CH_3CN employing a computer-controlled CHI660C electrochemical workstation, glassy carbon working electrode coated with FUIC or *i*-FUIC film, a platinum-wire auxiliary electrode, and an Ag/AgCl reference electrode. The potentials were referenced to a ferrocenium/ferrocene ($FeCp_2^{+/0}$) couple using ferrocene as an external standard. Thermogravimetric analysis measurements were performed using a thermogravimetric analyzer (Q600 TGA-DSC-DTA) under flowing nitrogen gas at a heating rate of 10 $^oC\ min^{-1}$. The thickness of active layer was measured on a Bruker DektakXT profilometer. The nanoscale morphology of the blended films was observed using a Multimode 8 scanning probe microscopy (Bruker) atomic force microscope (AFM) in the tapping mode. The grazing incidence X-ray scattering measurements (GIWAXS and GISAXS) were carried out with a Xeuss 2.0 SAXS/WAXS laboratory beamline using a Cu X-ray source (8.05 keV, 1.54 Å) and a Pilatus3R 300K detector. The incidence angle is 0.2°.

Molecular modelling.

Density functional theory (DFT) calculations were performed with the Gaussian 09 program,[S4] using the B3LYP functional.[S5, S6] All-electron double-ξ valence basis sets with polarization functions 6-31G* were used for all atoms.[S7] Geometry optimizations were performed with full relaxation of all atoms in gas phase without solvent effects. Vibration frequency calculation was performed to check that the stable structures had no imaginary frequency. Charge distribution of the molecules was calculated by Mulliken population analysis.

Fabrication and characterization of OSCs

The structure of regular OSCs was ITO/ZnO/PTB7-Th: acceptor/MoO_3/Ag. Patterned ITO glass (sheet resistance = 15 Ω $\square^{-1}$) was pre-cleaned in an ultrasonic bath with acetone and isopropanol, and treated in an ultraviolet–ozone chamber (Jelight Company, USA) for 2 min. ZnO layer (*ca.* 30 nm) was spin-coated at 4000 rpm onto the ITO glass from ZnO precursor solution (100 mg $Zn(CH_3COO)_2 \cdot 2H_2O$ and 0.02 mL ethanolamine dissolved in 1 mL 2-methoxyethanol), and then baked at 200 ^oC for 30 min. A PTB7-Th: acceptor mixture (12.5 mg mL^{-1} in total) in $CHCl_3$ was spin-coated at 1500 rpm on the ZnO layer to form a photoactive layer (*ca.* 100 nm). The MoO_3 layer (*ca*. 5 nm) and Ag electrode (*ca*. 80 nm) were slowly evaporated onto the surface of the photoactive layer under vacuum (*ca*. 10^{-5} Pa). The active area of the device was *ca.* 4 mm^2. The devices were not masked and the active area of devices was measured by optical microscopy. The *J–V* curve was measured using a computer-controlled B2912A Precision Source/Measure Unit (Agilent Technologies). An XES-70S1 (SAN-EI Electric Co., Ltd.) solar simulator (AAA grade, 70 × 70 mm^2 photobeam size) coupled with AM 1.5 G solar spectrum filters was used as the light source, and the optical power at the sample was 100 mW cm^{-2}. A 2 × 2 cm^2 monocrystalline silicon reference cell (SRC–1000-TC-QZ) was purchased from VLSI Standards Inc. The EQE spectrum was measured using Solar Cell Spectral Response Measurement System QE-R3011 (Enlitech Co., Ltd.). The light intensity at each wavelength was calibrated using a standard single crystal Si photovoltaic cell. For light stability test, we measured the photovoltaic performance of the unencapsulated devices under continuous AM 1.5G illumination at 100 mW cm^{-2} in glove box for a certain time.

Mobility measurements

Electron-only devices were fabricated using the architectures of Al/acceptor or PTB7-Th: acceptor/Al. Al (*ca*. 50 nm) was evaporated onto pre-cleaned glass under vacuum, acceptor or PTB7-Th: acceptor blend (*ca.* 100 nm) was spin-coated, and then Al (*ca.* 50 nm) was evaporated under vacuum. Hole-only devices were fabricated using the architectures of ITO/PEDOT: PSS/PTB7-Th: acceptor/Au. The pre-cleaned ITO glass was spin-coated with PEDOT: PSS (*ca*. 35 nm), then PTB7-Th: acceptor blend (*ca.* 100 nm) was spin-coated as active layer, then Au (*ca*. 30 nm) was evaporated under vacuum (*ca*. 10^{-5} Pa) at a low speed (1 Å/5 s) to avoid the penetration of Au atoms into the active layer. The mobility was extracted by fitting the current density–voltage curves using space charge limited current (SCLC).[S8] The equation is as follows:

$$J = (9/8)\mu\varepsilon_r\varepsilon_0 V^2 \exp(0.89(V/E_0L)^{0.5})/L^3$$

where J is current density, μ is hole or electron mobility, ε_r is relative dielectric constant, ε_0 is permittivity of free space, $V = V_{appl} - V_{bi}$, where V_{appl} is the applied voltage to the device, and V_{bi} is the built-in voltage due to the difference in work function of the two electrodes (for hole-only diodes, V_{bi} is 0.2 V; for electron-only diodes, V_{bi} is 0 V). E_0 is characteristic field, L is the thickness of organic layer. The J–V curves of the devices are plotted as $\ln[Jd^3/(V_{appl}-V_{bi})^2]$ *versus* $[(V_{appl}-V_{bi})/d]^{0.5}$.

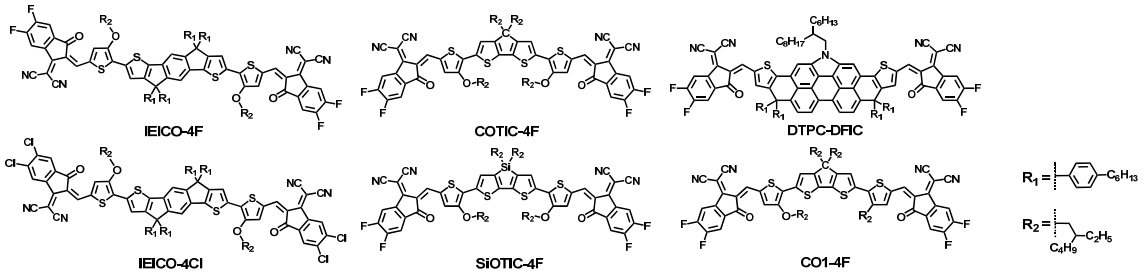

Fig. S1. Chemical structures of FREAs with an optical bandgap < 1.24 eV.

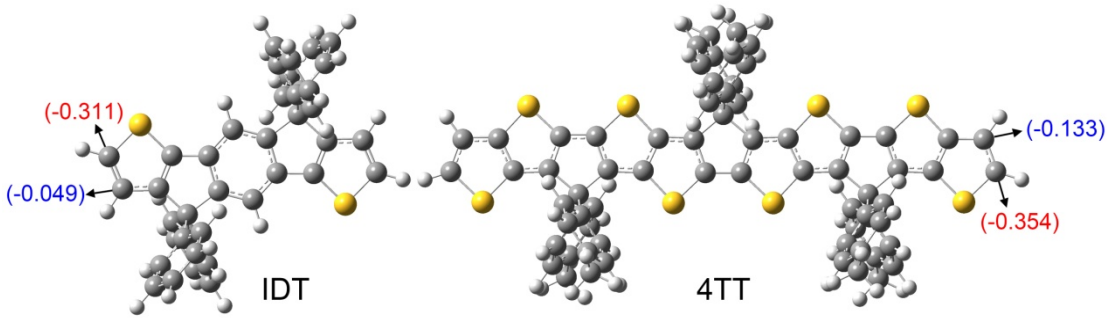

Fig. S2. Charges on the α- and β-carbons of IDT and 4TT.

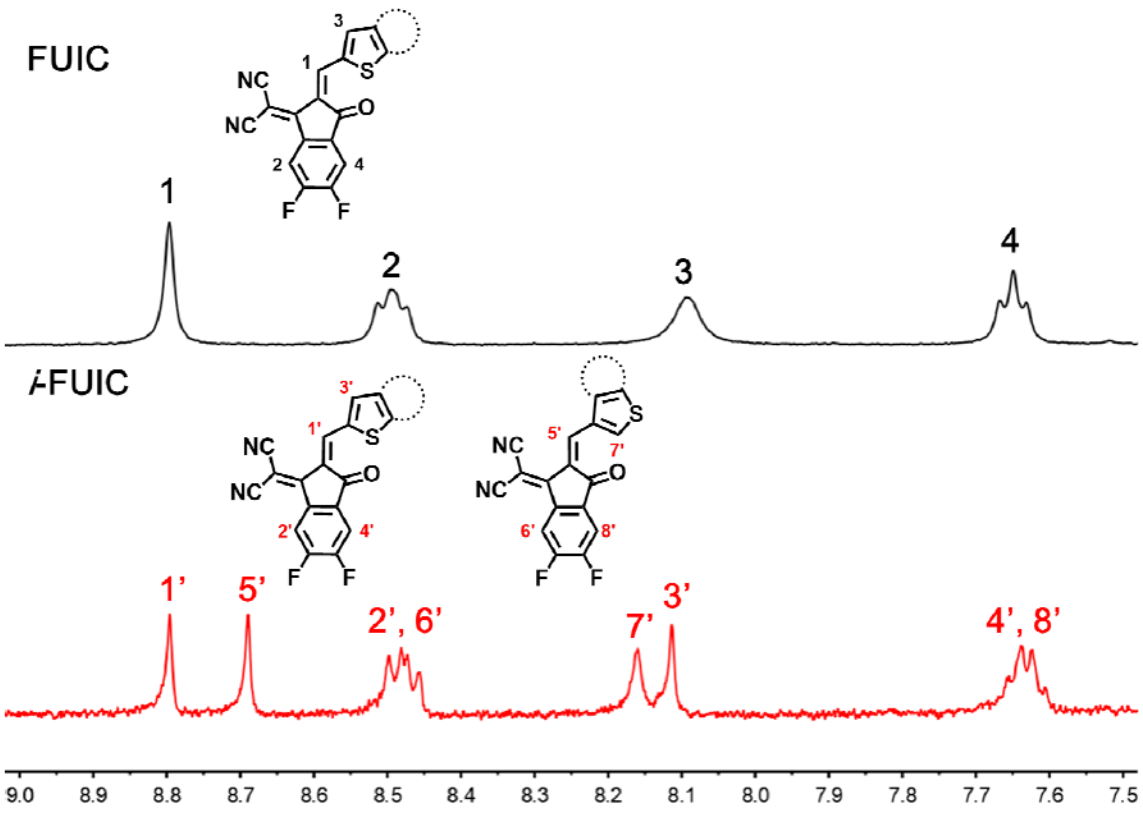

Fig. S3. Part of ^{1}H NMR spectra of FUIC and *i*-FUIC.

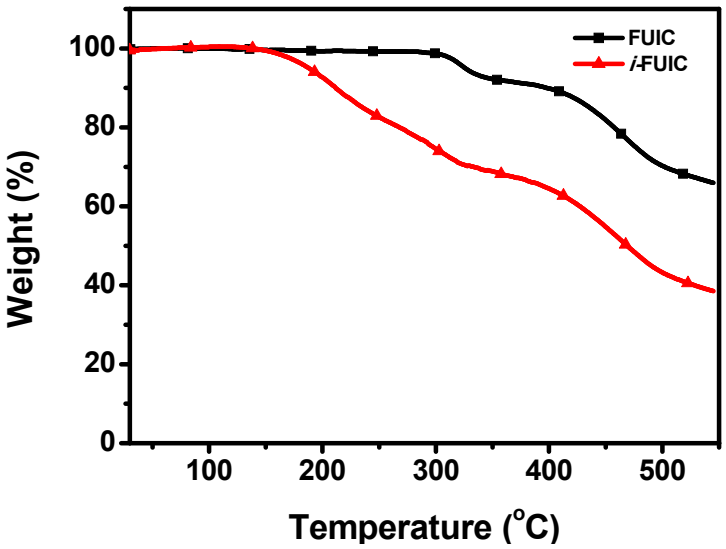

Fig. S4. TGA curves of FUIC and *i*-FUIC.

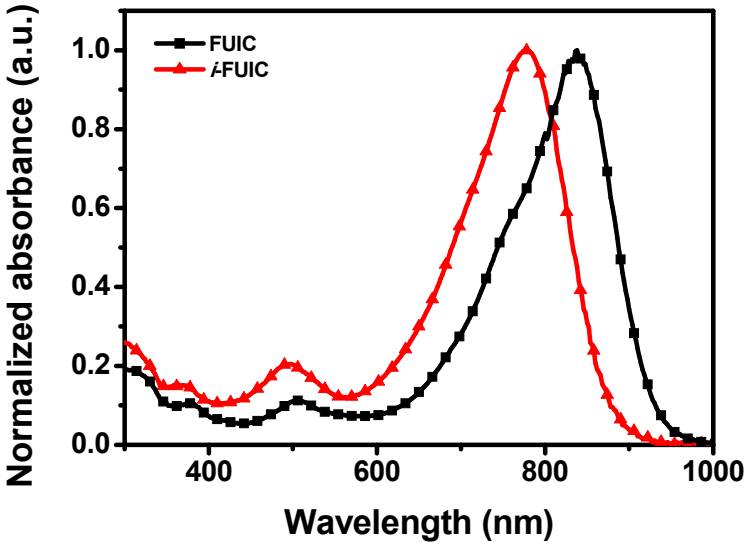

Fig. S5. Absorption spectra of FUIC and *i*-FUIC in chloroform solution.

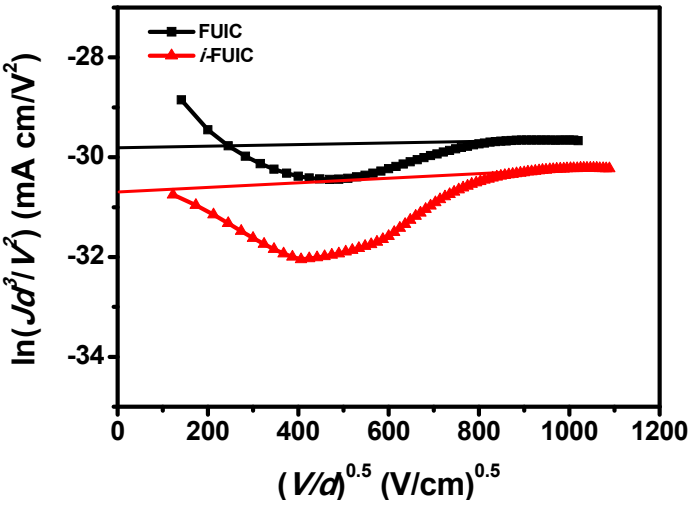

Fig. S6. *J-V* characteristics in the dark for electron-only devices based on FUIC and *i*-FUIC.

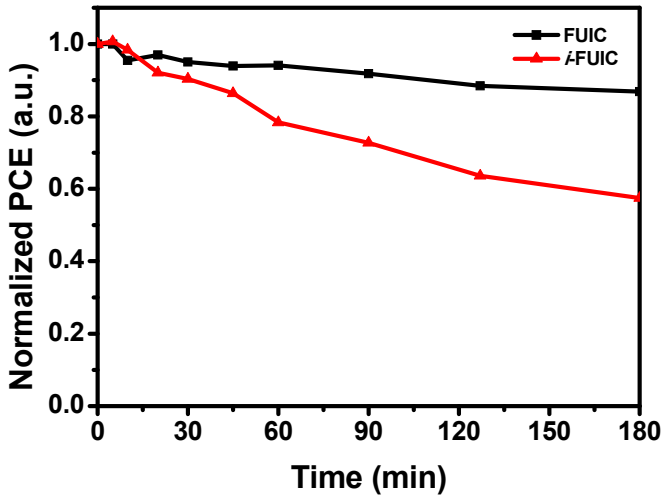

Fig. S7. Light stability of OSCs without encapsulation based on PTB7-Th: acceptor under continuous AM1.5G illumination at 100 mW cm^{-2}.

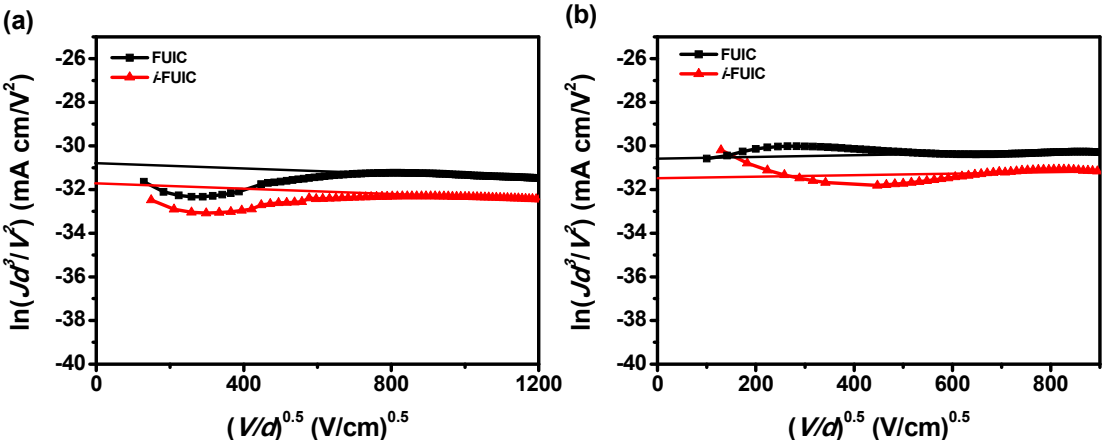

Fig. S8. *J-V* characteristics in the dark for (a) hole-only and (b) electron-only devices based on PTB7-Th: acceptor.

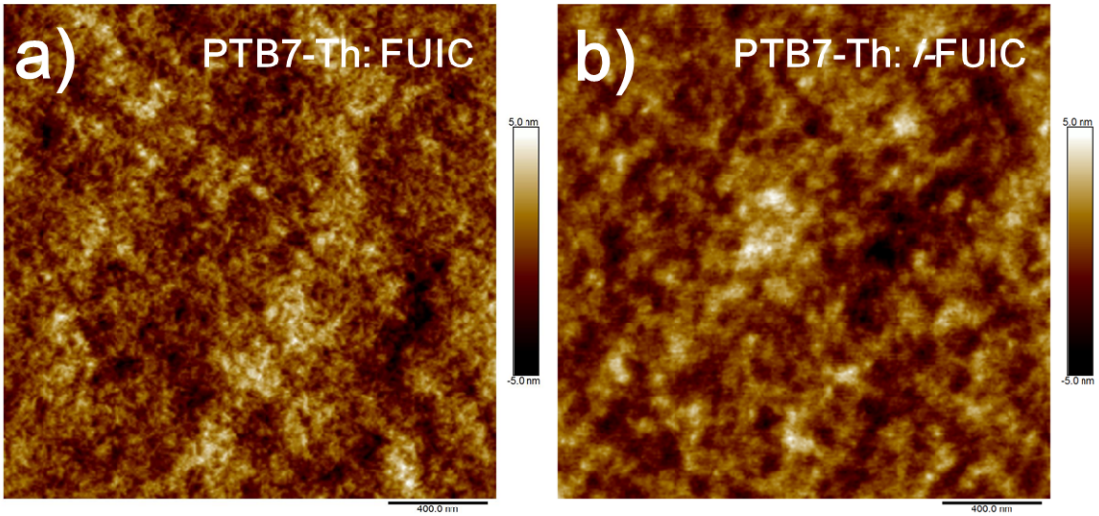

Fig. S9. AFM height images of PTB7-Th: acceptor blended films.

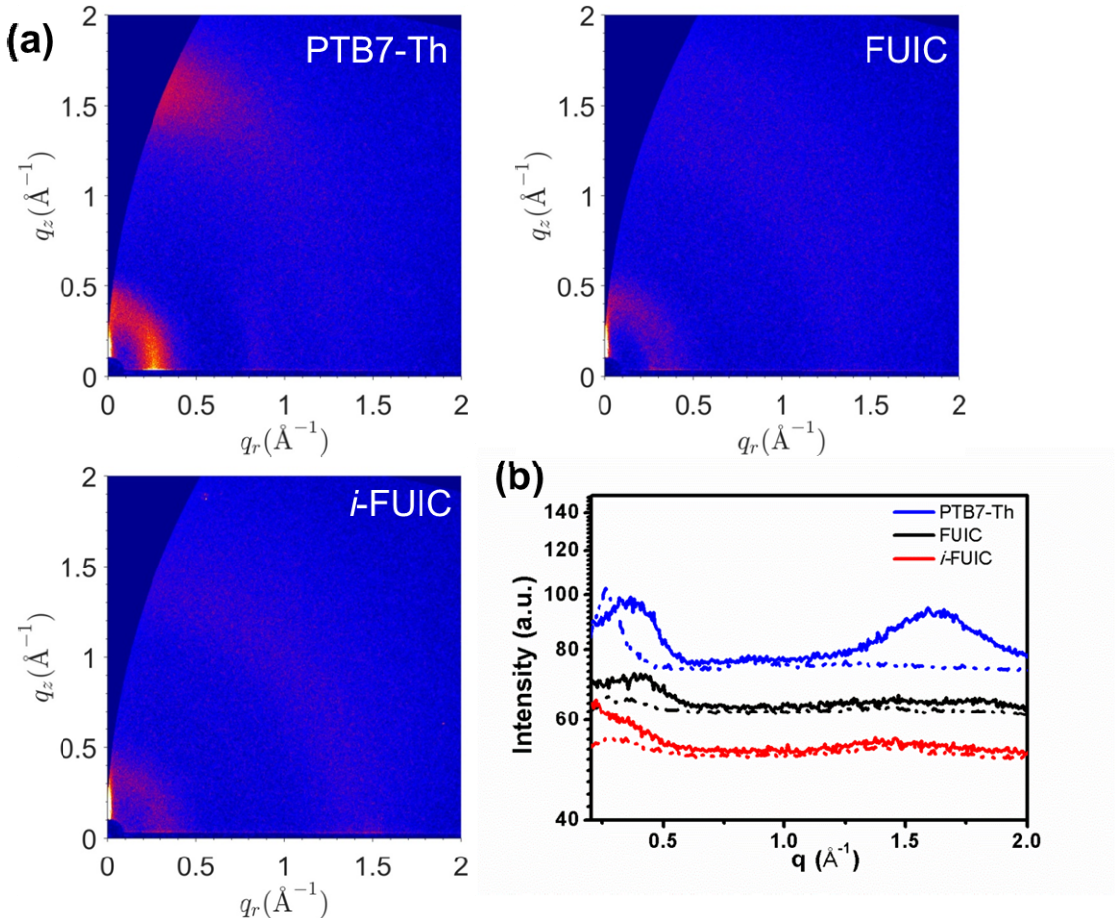

Fig. S10. (a) 2D GIWAXS patterns and (b) the scattering profiles of in-plane (dashed line) and out-of-plane (solid line) for PTB7-Th, FUIC and *i*-FUIC neat films.

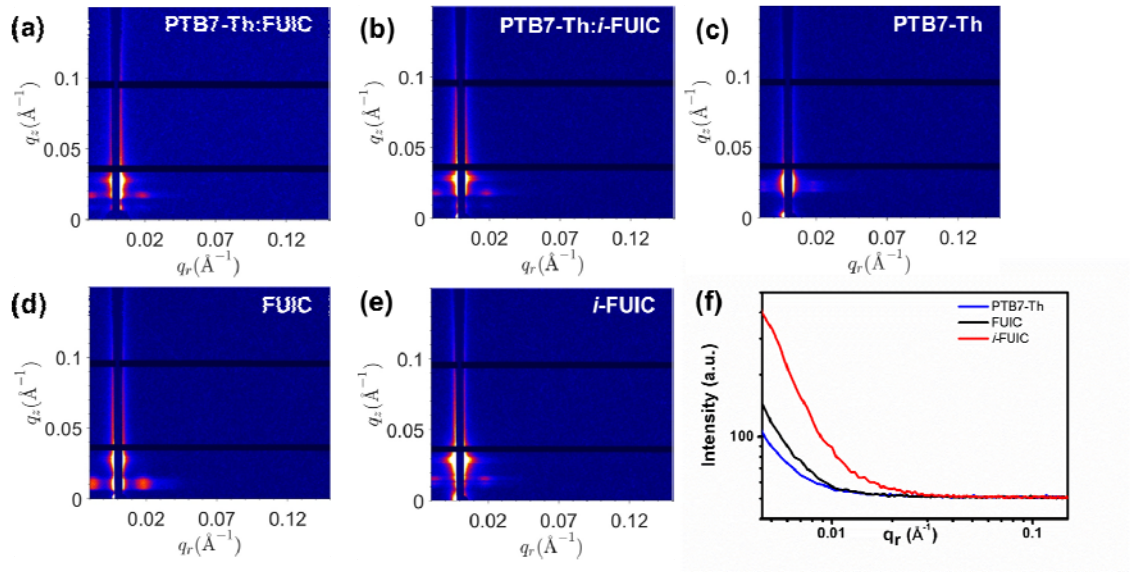

Fig. S11. 2D GISAXS patterns of (a, b) the blended films and (c, d, e) the PTB7-Th, FUIC and *i*-FUIC neat films, (f) the corresponding intensity profile of the pure donor and acceptors along the in-plane directions.

Table S1. The best performance of binary-blend OSCs based on acceptors with an optical bandgap < 1.24 eV.

Active layer	V_{OC} (V)	J_{SC} (mA cm^{-2})	FF (%)	PCE (%)	E_g[a] (eV)	Ref.
PBDTTT-EFT: IEICO-4F	0.739	22.8	59.4	10.0	1.24	S9
J52: IEICO-4F	0.734	21.9	58.5	9.4	1.24	S9
PTB7-Th: IEICO-4F	0.708	24.7	67.9	11.9	1.24	S10
PTB7-Th: IEICO-4Cl	0.727	22.8	62.0	10.3	1.23	S11
J52: IEICO-4Cl	0.700	23.8	60.7	10.1	1.23	S11
PBDB-T: IEICO-4Cl	0.744	20.8	62.5	9.67	1.23	S11
PTB7-Th: DTPC-DFIC	0.760	21.29	61.3	10.21	1.21	S12
PTB7-Th: SiOTIC-4F[b]	(0.65)	(21.6)	(61.4)	9.0 (8.6)	1.17	S13
PTB7-Th: COTIC-4F[b]	(0.56)	(20.3)	(56.3)	7.4 (6.4)	1.10	S13
PTB7-Th: CO1-4F	0.64	24.8	64	10.2	1.2	S14
PTB7-Th: FUIC	**0.692**	**22.9**	**70.6**	**11.2**	**1.22**	**This work**

[a] Estimated from the absorption edge in film. [b] The values in brackets are the average parameters.

Table S2. The optimization of the devices based on PTB7-Th: acceptor.

acceptor	D/A (w/w)	additive	annealing		V_{OC} (V)	J_{SC} (mA cm^{-2})	FF (%)	PCE (%)
			temperature (^{o}C)	time (min)				
FUIC	1:1.2	-	-	-	0.710	17.9	64.2	8.16
	1:1.5	-	-	-	0.713	18.9	64.6	8.71
	1:1.8	-	-	-	0.700	17.7	64.4	8.01
	1:1.5	0.5% CN	-	-	0.690	19.2	72.1	9.55
	1:1.5	1% CN	-	-	0.697	20.4	68.3	9.72
	1:1.5	2% CN	-	-	0.700	19.7	69.1	9.53
	1:1.5	1% CN	130	10	0.695	21.9	68.6	10.4
	1:1.5	1% CN	140	5	0.694	22.2	67.9	10.5
	1:1.5	1% CN	140	10	0.692	22.9	70.6	11.2
	1:1.5	1% CN	140	20	0.685	22.7	65.9	10.3
	1:1.5	1% CN	150	10	0.699	21.2	70.2	10.4
i-FUIC	1:1.2	-	-	-	0.781	19.7	55.3	8.51
	1:1.5	-	-	-	0.782	19.0	60.7	9.01
	1:1.8	-	-	-	0.778	18.5	60.9	8.76
	1:1.5	0.1% DIO	-	-	0.778	20.4	61.9	9.83
	1:1.5	0.2% DIO	-	-	0.782	20.9	63.0	10.3
	1:1.5	0.3% DIO	-	-	0.778	19.3	64.1	9.62

References

S1. J. Wang, J. Zhang, Y. Xiao, T. Xiao, R. Zhu, C. Yan, Y. Fu, G. Lu, X. Lu, S. R. Marder and X. Zhan, *J. Am. Chem. Soc.*, 2018, **140**, 9140-9147.

S2. S. Dai, F. Zhao, Q. Zhang, T. K. Lau, T. Li, K. Liu, Q. Ling, C. Wang, X. Lu, W. You and X. Zhan, *J. Am. Chem. Soc.*, 2017, **139**, 1336-1343.

S3. T. Li, S. Dai, Z. Ke, L. Yang, J. Wang, C. Yan, W. Ma and X. Zhan, *Adv. Mater.*, 2018, **30**, 1705969.

S4. M. J. Frisch, G. W. Trucks, H. B. Schlegel, G. E. Scuseria, M. A. Robb, J. R. Cheeseman, G. Scalmani, V. Barone, B. Mennucci, G. A. Petersson, H. Nakatsuji, M. Caricato, X. Li, H. P. Hratchian, A. F. Izmaylov, J. Bloino, G. Zheng, J. L. Sonnenberg, M. Hada, M. Ehara, K. Toyota, R. Fukuda, J. Hasegawa, M. Ishida, T. Nakajima, Y. Honda, O. Kitao, H. Nakai, T. Vreven, J. A. Montgomery Jr., J. E. Peralta, F. Ogliaro, M. J. Bearpark, J. Heyd, E. N. Brothers, K. N. Kudin, V. N. Staroverov, R. Kobayashi, J. Normand, K. Raghavachari, A. P. Rendell, J. C. Burant, S. S. Iyengar, J. Tomasi, M. Cossi, N. Rega, N. J. Millam, M. Klene, J. E. Knox, J. B. Cross, V. Bakken, C. Adamo, J. Jaramillo, R. Gomperts, R. E. Stratmann, O. Yazyev, A. J. Austin, R. Cammi, C. Pomelli, J. W. Ochterski, R. L. Martin, K. Morokuma, V. G. Zakrzewski, G. A. Voth, P. Salvador, J. J. Dannenberg, S. Dapprich, A. D. Daniels, Ö. Farkas, J. B. Foresman, J. V. Ortiz, J. Cioslowski and D. J. Fox, Gaussian 09, Revision A.01 ed., Gaussian, Inc., Wallingford CT, USA, 2009.

S5 A. D. Becke, *Phys. Rev. A* 1988, **38**, 3098-3100.

S6 C. Lee, W. Yang and R. G. Parr, *Phys. Rev. B* 1988, **37**, 785-789.

S7 R. Krishnan, J. S. Binkley, R. Seeger and J. A. Pople, *J. Chem. Phys.* 1980, **72**, 650-654.

S8. G. G. Malliaras, J. R. Salem, P. J. Brock and C. Scott, *Phys. Rev. B* 1998, **58**, 13411.

S9. H. Yao, Y. Cui, R. Yu, B. Gao, H. Zhang and J. Hou, *Angew. Chem. Int. Ed.*, 2017, **56**, 3045-3049.

S10. Y. Cui, H. Yao, C. Yang, S. Zhang and J. Hou, *Acta Polym. Sin.* 2018, **2**, 223.

S11. Y. Cui, C. Yang, H. Yao, J. Zhu, Y. Wang, G. Jia, F. Gao and J. Hou, *Adv. Mater.*, 2017, **29**, 1703080.

S12. Z. Yao, X. Liao, K. Gao, F. Lin, X. Xu, X. Shi, L. Zuo, F. Liu, Y. Chen and A. K. Jen, *J. Am. Chem. Soc.*, 2018, **140**, 2054-2057.

S13. J. Lee, S. J. Ko, M. Seifrid, H. Lee, B. R. Luginbuhl, A. Karki, M. Ford, K. Rosenthal, K. Cho, T. Q. Nguyen and G. C. Bazan, *Adv. Energy Mater.*, 2018, **8**, 1801212.

S14. J. Lee, S.-J. Ko, H. Lee, J. Huang, Z. Zhu, M. Seifrid, J. Vollbrecht, V. V. Brus, A. Karki, H. Wang, K. Cho, T.-Q. Nguyen and G. C. Bazan, *ACS Energy Lett.*, 2019, **4**, 1401-1409.